The Band Spectrum of Sulphur Monoxide

By Emmett V. Martin

University of California, Berkeley, California

(Received May 16, 1932)

The spectrum of SO, which lies in the region 2400–4000A, has been photographed in the 2nd order of a 21-foot grating. The wave-numbers of the lines of the seven bands, (0,4), (0,5), (0,6), (0,7), (0,8), (0,9), and (1,4), are tabulated.

Rotational structure.—The analysis of the rotational structure leads to the assignment of the band system to a $^3\Sigma$, $^3\Sigma$ electronic transition, and yields the following values of the constants:

$r_e' = 1.769 \times 10^{-8}$ cm $r_e'' = 1.489 \times 10^{-8}$ cm $D_e' = -1.280 \times 10^{-6}$ cm^{-1}

$I_e' = 55.10 \times 10^{-40}$ gr. cm^2 $I_e'' = 39.02 \times 10^{-40}$ gr. cm^2 $\beta' = -3.56 \times 10^{-9}$ cm^{-1}

$B_e' = 0.5020 \pm 0.0005$ cm^{-1} $B_e'' = 0.70894 \pm 0.00009$ cm^{-1} $D_e'' = -1.129 \times 10^{-6}$ cm^{-1}

$\alpha_e' = 0.0062$ cm^{-1} $\alpha_e'' = 0.00562 \pm 0.000013$ cm^{-1} $\beta'' = -3.20 \times 10^{-10}$ cm^{-1}

Spin fine-structure. The triplets are resolved for $K > 30$ and for $K < 13$. However, due to overlapping of the different branches, the resolution for $K < 13$ could be observed well in the (0,8) band only. It was found that, in order to represent adequately the observed separations of the triplets, it was necessary to modify somewhat the equations in Kramers' theory of spin tripling in $^3\Sigma$ states. The equations which best respresent the data are:

$$\Delta_{2-1} = A - B/(2K+3) - (\gamma' - \gamma'')(K+1)$$

$$\Delta_{2-3} = A + B/(2K-1) + (\gamma' - \gamma'')K$$

where, for the (0,8) band, $A = -2.11$, $B = -10.83$, and $(\gamma' - \gamma'') = +0.0150$. Of these three constants, A is the only one which is different for different bands; it ranges from -1.97 for the (0,4) band to -2.19 for the (0.9) band. We cannot determine which one, if either, of the two terms, A and B, represents the value of $3(\epsilon' - \epsilon'')$ in Kramers' theory. The values of $\Delta_2 F_1(K)$ and $\Delta_2 F_3(K)$ indicate that $\gamma' \sim +0.017$ and that $\gamma'' \sim -0.003$.

Predissociation and perturbations. Bands with $v' = 0, 1, 2,$ and 3 are observed to break off at $K' = 66$, 53, 39, and 6, respectively. No bands with $v' > 3$ are observed. This effect is explained as predissociation, and is assumed to be caused by a $^3\Pi$ state. Not only do the rotational levels for different v' end at different values of K', but also the term value at which the break occurs decreases with increasing v'. If the potential energy curve for the $^3\Pi$ state is assumed to have a shallow minimum, a satisfactory explanation of the effect of rotation on predissociation is obtained by an application of Oldenberg's theory of dissociation by rotation. A further indication that the $^3\Pi$ potential energy curve has a shallow minimum is given by the observed perturbations of the rotational levels of the upper $^3\Sigma$ state. According to our interpretation, the term value at which the rotational levels for $v' = 3$ terminate corresponds to dissociation of the normal state of the SO molecule. The energy of dissociation of this state, measured from the $v'' = 0$ vibrational level, is calculated to be 5.053 ± 0.001 volts.

Vibrational structure. The origins of several bands of the $v' = 0$ progression are calculated, and the vibrational constants of the lower state determined from them. Since the bands with $v' > 1$ are too much perturbed to permit an analysis of their rotational structure, it was necessary to use measurements of band heads to determine the vibrational constants of the upper state. The constants obtained are: $\omega_e'' = 1123.73 \pm 0.24$ cm^{-1}, $x_e'' \omega_e'' = 6.116 \pm 0.017$ cm^{-1}, $\omega_e' = 628.7$ cm^{-1}, and $x_e' \omega_e' = 5.65$ cm^{-1}.

I. Introduction

THE sulphur monoxide band spectrum, which appears in the region 4000 to 2400A, was first described in 1906 by Miss Lowater.[1] A more complete study of this spectrum was made in 1924 by Johnson and Cameron,[2] who arranged the bands in series. In 1929, Henri and Wolff[3] photographed this system with a quartz-prism Littrow spectrograph, made the vibrational analysis, and assigned the spectrum to the molecule SO. As shown below, there is good evidence that their assignment of vibrational quantum numbers is correct; hence it has been used in this work. Because of insufficient dispersion, however, they were able to make only a partial analysis of the rotational structure. From the average second differences of the frequencies of the unresolved P and R series in a number of bands with $v' = 0$, they evaluated the constant α'', which is defined by the relation:[3a]

$$B_v'' = B_e'' - \alpha''(v'' + \tfrac{1}{2}). \tag{1}$$

In order to determine B_e'', they then substituted α'' into the equation:

$$\alpha''\omega_e'' = 6B_e''^2 \tag{2}$$

where ω_e'' is the frequency of vibration for infinitesimal amplitude; ω_e'' was known from the analysis of the vibrational structure of the system.

Eq. (2) results from a special form[4] of the function assumed by Kratzer[5] for the potential energy of a diatomic molecule. This function can be written:

$$U = 2k(\tfrac{1}{2} - 1/\rho + 1/2\rho^2 - c_3\xi^3 - c_4\xi^4), \tag{3}$$

where $\rho = r/r_e$, $\xi = \rho - 1$, and k, c_3, and c_4 are constants. It can be shown that[4]

$$c_3 = \tfrac{1}{2}(\alpha\omega_e/6B_e^2 - 1), \text{ and } c_4 = (x_e\omega_e/3B_e - 1) - \tfrac{1}{2}5c_3(c_3 + 2), \tag{4}$$

where $x_e\omega_e$ is the coefficient of the second degree term in the expression for the vibrational term values. If c_3 and c_4 are set equal to zero, Eq. (2) follows. Birge[6] has calculated the values of c_3 and c_4 for the electronic states of a number of different molecules, and has found that, if they are neglected as in Eq. (2), values of B_e are obtained which are in some cases in error by as much as 50 percent. Therefore, it seemed likely that the value of B_e'' given by Henri and Wolff represented only the order of magnitude of the correct value.

Henri and Wolff concluded that the band structure consisted of a Q branch only, the lines of which were narrow multiplets. This type of structure appeared to be in marked contrast with that of the known band systems

[1] Frances Lowater, Ast. Jour. **23**, 324 (1906).

[2] R. C. Johnson and W. H. B. Cameron, Proc. Roy. Soc. **A106**, 195 (1924).

[3] V. Henri and F. Wolff, Jour. Phys. Rad. **10**, 81 (1929).

[3a] The notation used in this paper is that agreed upon by leading spectroscopists, as reported by R. S. Mulliken, Phys. Rev. **36**, 611 (1930).

[4] W. Weizel, Handbuch der Experimentalphysik, Ergänzungswerk, Band I, (1931). A.E Ruark and H. C. Urey, *Atoms, Molecules, and Quanta* (1930).

[5] A. Kratzer, Zeits. f. Physik **3**, 289 (1920).

[6] R. T. Birge, Unpublished work.

of O_2[7,8] and S_2[9] which lie in the same spectral region as the SO bands. Since these systems of O_2 and S_2 are quite similar, in that both result from the same type of electronic transition, it was expected that this system of SO would also have similar characteristics. In view of these uncertainties, it was considered to be of value to obtain new spectrograms under higher dispersion in an attempt to obtain unambiguous values of the molecular constants, and to clarify the apparently anomalous rotational structure.

II. EXPERIMENTAL PROCEDURE

In the investigation by Henri and Wolff, the spectrum was excited by passing a spark discharge between small aluminum rods in a quartz bulb containing SO_2 at a pressure of 30–40 mm. A quartz window was placed close to the spark to avoid the absorption by SO_2 which occurs in the same spectral region as the SO bands. This method had the disadvantages that an exposure
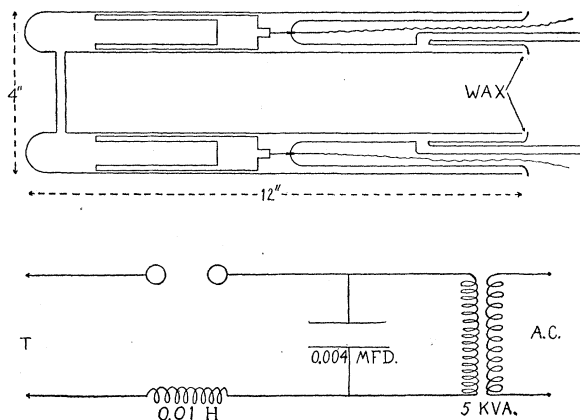
Fig. 1. Upper; diagram of the quartz discharge tube. The light was taken from the side of the constricted ($\frac{1}{4}''$ diameter) portion of the tube. Lower, schematic diagram of the electrical circuit. The leads marked T connect to the discharge tube.

of several hours was required even with a quartz spectrograph, and that it was necessary to interrupt exposure frequently in order to remove deposits of sulphur from the window and to allow the tube to cool.

A diagram of a discharge tube which does not have these disadvantages is shown in Fig. 1. This tube was constructed entirely of quartz, and was connected to the glass system by means of the wax seals shown. These seals were far enough removed from the discharge so that they were not overheated. The electrodes were heavy aluminum cylinders. A P_2O_5 drying tube, a liquid-air trap, and a two-liter flask comprised the remainder of the system. SO_2 was taken from a tank and frozen in the liquid-air trap; the system was then evacuated and allowed to fill with SO_2 to a pressure of about 20 mm. The two liter flask was necessary as a reservoir, because, even with this much volume.

[7] W. Ossenbrüggen, Zeits. f. Physik **49**, 167 (1928).

[8] W. Lochte-Holtgreven and G. H. Dieke, Ann. d. Physik **3**, 937 (1929).

[9] S. M. Naude and A. Christy, Phys. Rev. **37**, 490 (1931).

the pressure in the system would fall several millimeters in an hour, due to the removal of SO_2 by the deposition of sulphur on the walls of the tube and to the oxidation of the electrodes. The SO_2 could then be replenished from the liquid-air trap supply.

If the light was taken from the side of the constricted portion ($\frac{1}{4}''$ diameter) of the tube, there was no appreciable absorption by SO_2, and the heat produced by the discharge itself prevented the deposition of sulphur on this constricted part. Previous trials had shown the impossibility of using a tube of the "end-on" type, with which these difficulties could not be avoided.

The tube adopted therefore required no interruption of exposure to be cooled or cleaned, and, when excited with a heavy current, produced a comparatively high intensity of the spectrum.

The electrical circuit also is shown in Fig. 1. The transformer was actuated by a potential of 220 volts, and had an open-circuit secondary voltage of 10 kilovolts and a capacity of 5 k.v.a. The condenser consisted of two Leyden jars in parallel, and the self-inductance coil was constructed by winding No. 24 D.C.C. copper wire in a single layer on a long paper cylinder. Henri and Wolff showed that this type of circuit was practically necessary for the production of the spectrum with any intensity. An ordinary uncondensed discharge produces the band spectrum, but most of the energy goes into the production of a continuous spectrum in the same spectral region. On the other hand, a condensed discharge produces the line spectrum only. The optimum values of capacity and inductance are indicated in Fig. 1; they could not be changed from these values by a factor of more than about five without a change in the spectrum becoming noticeable.

The intensity of the spectrum was also dependent upon the pressure in the tube; it increased with increasing pressure up to about 2 cm, but appeared to remain practically constant for pressures above this value. The power applied to the tube was controlled by regulating the primary voltage of the transformer. To obtain the maximum intensity, the power was adjusted to the maximum value at which the tube could operate continuously. This value is estimated to be about 2 k.w.

The spectrograms used for measurement were taken on Eastman Speedway plates in the first and second orders of a 21-foot grating which has a dispersion in the second order of about 1.3 A/mm. The exposure time required was six hours. The lines were measured with a Société Genévoise comparator reading to 0.001 mm. The lines of an iron arc in air were used as comparison standards. The wave-lengths used were taken from the "Transactions of the International Astronomical Union"[10] and the "Publications of the Allegheny Observatory of the University of Pittsburgh."[11] The former gives values for the arc in air, the latter for the arc in vacuum. Unfortunately, no International standard wave-lengths are available for the region below 3370A. However, the two sources agreed very closely for the wave-lengths which they both give; hence it was assumed that there was no appreciable error intro-

[10] Transactions of the International Astronomical Union, Vol. III, (1929).

[11] Publications of the Allegheny Observatory of the University of Pittsburgh, Vol. VI (1929).

duced by using for some of the standards the wave-lengths of the lines of the vacuum iron arc. The deviations of these lines from a smooth dispersion curve indicated that the SO band lines were measured with an absolute accuracy of about 0.01A, while combination relations showed for the sharper lines a relative accuracy within a band of about 0.003A.

III. ROTATIONAL STRUCTURE

The general appearance of the spectrum is shown in Fig. 2, a and b. The progression with $v' = 0$ is predominant, and its most intense members, namely the (0, 4) to (0, 9) bands inclusive, are almost entirely free from overlapping by other bands of the system. These bands were therefore most suitable for the determination of the molecular constants. The constants of the lower states having $v'' = 4$ to 9, and of the upper state having $v' = 0$, could be accurately determined from these bands, while for the upper state having $v' = 1$, the (1, 4) band was found to be most suitable. No bands with $v' > 1$ could be used for this purpose; those with $v' = 2$ were too much perturbed to permit an analysis of their structure, while those with $v' = 3$ were extremely narrow, an effect which is explained below as due to predissociation. No bands with $v' > 3$ are observed, also because of predissociation.

The structure of the bands with $v' = 0$ is illustrated in Fig. 2, d and f, which show enlargements of the (0, 7) and (0, 5) bands respectively. These bands show one R and one P branch, each of which consists of narrow triplets. The two high-frequency components (to left in Fig. 2) of the triplets have a frequency separation which is dependent on the value of K, while the separation of the low-frequency member from the mean of the two high-frequency members is nearly independent of K. The absence of any noticeable Q branches indicates that the transition is one for which $\Delta\Lambda = 0$. Furthermore, because of the considerable intensity of the system, the possibility of an intersystem transition ($\Delta S \neq 0$) can be ruled out. Since no Λ-type doubling is observed, both states must have $\Lambda = 0$. The presence of triplet R and P branches shows that the electronic states involved belong to a triplet system. These facts point quite definitely to the conclusion that this band system is produced by a $^3\Sigma$, $^3\Sigma$ transition, as is the case for the analogous systems of O_2[7,8] and S_2[9] lying in the same spectral region. Since the final $^3\Sigma$ states for these systems of O_2 and S_2 are the normal states of these molecules, the final $^3\Sigma$ state for this system of SO is probably also the normal state.

The complete resolution of the spin tripling is one of the most interesting features of the SO bands. In the corresponding bands of O_2, the tripling is much smaller, and the components arising from F_1 and F_3 terms are barely resolved at the highest observed K values. In S_2, although the triplet separations are as large as in SO, overlapping is so serious that the data are irregular and incomplete.

The rotational levels of a Σ state are given by[12]

$$F_i(K) = B_v K(K + 1) + f_i(K, J - K) + D_v K^2(K + 1)^2 + \cdots \qquad (5)$$

[12] For details, see R. S. Mulliken, Rev. Mod. Phys. **2**, 105 (1931). The factor $\overline{G^2}$ has been omitted from Eq. (5).

where K is the quantum number of the angular momentum exclusive of spin, J is the quantum number of the total angular momentum and takes the values $J = K + S$, $K + S - 1$, $\cdots$, $K - S$, and S is the resultant spin. For a triplet state, $S = 1$; hence, for this case, $J = K + 1$, K, and $K - 1$. Since the difference in energy for different orientations of spin is small for Σ states (Hund's case (b)), there will be, in this case, three rather closely spaced en-
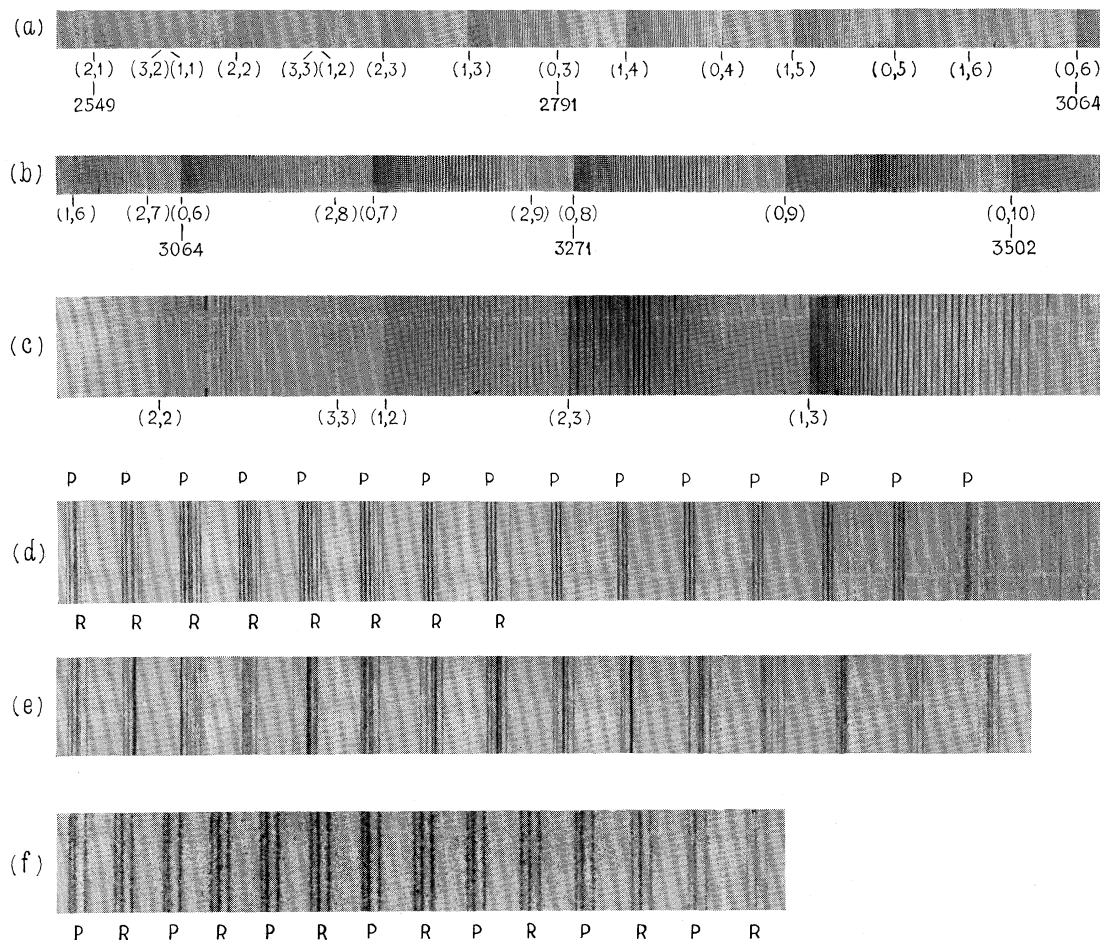
Fig. 2. Reproduction of the major parts of the SO emission spectrum, photographed with a 21-foot grating. (a) and (b). Contact prints of the region $\lambda 2500A$ to $\lambda 3550A$, which contains most of the stronger bands. (c). Enlargement of the short wave-length end of the spectrum to show the abrupt termination of the bands with $v' = 2$ and $v' = 3$. This is especially well illustrated by the 2,2 band. The 3,3 band is probably too faint to show in the reproduction, but actually is only about 1 mm wide. (d). Enlargement of the end of the 0,7 band showing the abrupt ending of the R and P branches. (e). Enlargement of part of the 1,4 band illustrating the perturbations in the rotational structure. (f). Enlargement of part of the 0,5 band. The complete resolution of the triplets and their different relative spacing for adjacent lines, $R(K)$ and $P(K-6)$, are apparent.

ergy states for each value of K. These energy states are designated $F_i = F_1$, F_2, and F_3, where F_1 corresponds to $J = K+1$, F_2 to $J = K$, and F_3 to $J = K-1$.

Kramers[13] has shown that $f_i(K, J-K)$ for $^3\Sigma$ states is made up of two parts, one of which is due to the interaction of the resultant electron spin $S^*(=(S(S+1))^{\frac{1}{2}})$ and the magnetic field generated by the rotation of the nuclei, while the other is due to the interaction of the individual spins of the electrons. For the three values of J, $f_i(K, J-K)$ is given by

$$J = K + 1 \qquad f_1 = -\epsilon + 3\epsilon/(2K + 3) + \gamma K \qquad (6)$$
$$J = K - 1 \qquad f_3 = -\epsilon - 3\epsilon/(2K - 1) - \gamma(K + 1) \qquad (7)$$
$$J = K \qquad f_2 = +2\epsilon - \gamma. \qquad (8)$$

In these equations, terms containing γ arise from the interaction of the resultant spin and the magnetic field generated by the nuclear rotation, and those containing ϵ arise from the interaction of the individual spins.

The lines of the R and P branches are defined by the relations:

$$R_i(K) = \nu_0 + F_i'(K + 1) - F_i''(K) \qquad (9)$$
$$P_i(K) = \nu_0 + F_i'(K - 1) - F_i''(K) \qquad (10)$$

where ν_0 is the wave-number of the origin of the band under consideration.

In the analysis of a $^3\Sigma$, $^3\Sigma$ band system, it is impossible to determine the signs of the γ's and ϵ's. This fact prevents an unambiguous assignment of all three R (or P) branches to the series R_1, R_2, and R_3 (or P_1, P_2, and P_3). From the fact that f_2 is independent of K, we can identify the R_2 (or P_2) branch at once, but we cannot determine which of the other two R (or P) branches is R_1 (or P_1). In the present case, the low-frequency branch is R_2 (or P_2), while the high-frequency branch (for $K > 18$) has been arbitrarily designated as R_1 (or P_1), by analogy with the corresponding convention used for S_2[9]. Table I gives the wave-numbers of the lines of the seven bands investigated. The lines indicated by asterisks are unresolved R_1 and R_3 (or P_1 and P_3) lines. The order in which the three branches are given in the table is, reading downward: R_1, R_3, R_2 (or P_1, P_3, P_2). This order is maintained for all of the bands with $v' = 0$, and also for the (1,4) band up to $K = 25$. For $K > 25$, however, the (1,4) band is so much perturbed that it was impossible to arrange the R (or P) branches into three distinct series. The wave-length in I.A. of the head of each band is given at the top of the appropriate columns.

The correct designation of the lines by the values of K'' was obtained by the application of the combination principle. After a few preliminary trials, assignments were reached which yielded, for all bands with a common upper vibrational state, complete agreement in the term differences

$$\Delta_2 F_i'(K) = R_i(K) - P_i(K) = F_i'(K + 1) - F_i'(K - 1).$$

For the three components of the triplet, these differences should be given by:[14]

$$\Delta_2 F_1'(K) = 4B_v'(K + \tfrac{1}{2}) + 8D_v'(K + \tfrac{1}{2})^3 - 12\epsilon'/(2K + 5)(2K + 1) + 2\gamma' \quad (11)$$
$$\Delta_2 F_3'(K) = 4B_v'(K + \tfrac{1}{2}) + 8D_v'(K + \tfrac{1}{2})^3 + 12\epsilon'/(2K - 3)(2K + 1) - 2\gamma' \quad (12)$$
$$\Delta_2 F_2'(K) = 4B_v'(K + \tfrac{1}{2}) + 8D_v'(K + \tfrac{1}{2})^3. \quad (13)$$

---

[13] H. A. Kramers, Zeits. f. Physik **53**, 422 (1929).

[14] The omission of a term $+6D_v(K+\tfrac{1}{2})$ from these equations introduces no appreciable error, since $6D_v$ is entirely negligible in comparison with $4B_v$.

TABLE I. *Wave numbers of the lines of the (1, 4), (0, 4), (0, 5), (0, 6), (0, 7), (0, 8), and (0, 9) bands.*

K''	(1, 4) λ2827.395 R	P	(0, 4) λ2877.643 R	P	(0, 5) λ2968.470 R	P
7	—	35336.56*	—	34719.20*	—	33657.37*
	—	335.55	—	—	—	—
8	—	—	—	715.47*	—	653.36*
	—	331.38	—	—	—	—
9	—	—	—	711.20*	—	649.70*
	—	326.94	—	—	—	—
10	—	323.35*	—	706.57*	—	645.18*
	—	322.05	—	—	—	—
11	—	318.10*	34724.59*	701.61*	—	640.54*
	—	316.50	722.67	—	—	637.58
12	35337.35*	312.77*	721.13*	696.25*	—	634.53*
	335.55	310.86	719.20	694.13	—	632.18
13	333.28*	306.76*	717.41*	690.48*	33655.71*	628.84*
	331.38	304.84	715.47	688.41	653.85	626.79
14	328.99*	300.40*	713.10*	684.20*	651.74*	623.07*
	326.94	298.38	711.20	682.19	649.70	620.80
15	324.27*	293.73*	708.60*	677.68*	647.39*	616.51*
	322.05	291.72	706.57	675.64	645.18	614.49
16	319.12*	286.66*	703.60*	670.78*	642.67*	609.80*
	317.12	284.64	701.61	668.71	640.54	607.79
17	313.66*	279.16*	698.32*	663.47*	637.58*	602.68*
	311.65	277.16	696.25	661.44	635.52	600.61
18	307.69*	271.33*	692.66*	655.80*	632.18*	595.25*
	305.71	269.34	690.48	653.76	630.06	593.23
19	301.46*	262.96*	686.61*	647.76*	626.32*	587.42*
	299.54	261.07	684.56	645.64	624.33	585.39
20	294.94*	253.59*	680.21*	639.41*	620.07*	579.28*
	292.86	252.50	678.22	637.42	618.08	577.25
21	287.86*	245.31*	673.42*	630.62*	613.54*	570.69*
	285.86	243.52	671.45	628.64	611.47	568.66
22	280.41*	236.28*	666.33*	621.45*	606.65*	561.84*
	278.28	234.16	664.33	619.54	604.57	559.86
23	35272.64*	35226.26*	34658.75*	34612.00*	33599.32*	33552.57*
	270.05	224.31	656.74	610.01	597.26	550.54
24	264.36*	215.97*	650.83*	602.13*	591.74*	543.01*
	262.96	214.15	648.90	600.13	589.69	541.00
25	255.48*	205.77*	642.58*	591.88*	583.81*	533.07*
	254.36	203.06	640.59	589.83	581.75	531.00
26	247.66*	194.79*	633.95*	581.30*	575.45*	522.71*
	245.31	193.14	632.11	579.32	573.52	520.71
27	238.04	185.36	625.23	570.29*	567.02	512.03*
	—	183.20	624.73	—	466.48	—
	235.78	181.94	623.01	568.25	564.71	510.01
28	228.54	172.52	615.82	559.16	557.92	501.03*
	—	—	615.34	558.72	557.43	—
	226.26	170.16	613.60	557.07	555.68	499.18
29	218.16	160.35	606.07	547.51	548.57	489.68*
	—	—	605.54	547.02	548.02	—
	214.15	158.05	603.86	545.30	546.23	487.65
30	207.42	148.12	596.06	535.41	538.76	478.16
	—	—	595.38	534.87	538.23	477.69
	206.61	145.56	593.64	533.16	537.42	475.90
31	197.37	135.03	585.48	523.04	528.63	466.04
	196.66	—	584.89	522.47	528.01	465.46
	194.79	132.58	583.17	520.70	526.35	463.78
32	185.97	121.73	574.64	510.15	518.16	453.62
	185.36	—	573.99	509.54	517.54	453.04
	181.94	120.67	572.32	507.86	515.79	451.33
33	175.13	108.65	563.41	497.00	507.34	440.78
	173.08	108.06	562.72	496.36	506.75	440.22
	171.66	106.21	561.10	494.58	504.97	438.49

TABLE I. (*Cont.*).

K''	(1, 4) R	P	(0, 4) R	P	(0, 5) R	P
	160.35	094.35	551.85	483.39	496.10	427.60
34	—	—	551.10	482.72	495.45	427.00
	—	090.84	549.44	481.05	493.66	425.27
	150.33	081.18	539.87	469.44	484.49	414.12
35	149.74	079.14	539.08	468.70	483.76	413.45
	148.12	077.78	537.46	467.16	482.11	411.75
	137.48	063.82	527.56	455.16	472.56	400.21
36	136.84	—	526.85	454.45	471.88	399.57
	135.03	—	525.08	452.76	470.18	397.85
	35123.69	35050.98	34514.85	34440.49	33460.32	33385.93
37	—	050.34	514.03	439.76	459.48	385.34
	121.73	048.67	512.35	438.10	457.84	383.56
	110.91	035.47	501.69	425.47	447.63	371.37
38	109.96	034.81	500.86	424.78	446.80	370.63
	108.65	033.15	499.21	423.03	445.14	368.87
	097.02	018.98	488.24	410.07	434.58	356.44
39	095.82	—	487.37	409.21	433.71	355.56
	094.35	017.26	485.77	407.58	432.10	353.96
	082.60	003.44	474.41	394.20	421.21	341.05
40	—	002.58	473.43	393.44	420.26	340.21
	080.39	001.27	471.95	391.82	418.71	338.56
	067.23	34986.83	460.12	378.00	407.39	325.41
41	—	985.74	459.25	377.22	406.52	324.47
	065.26	984.32	457.70	375.59	404.93	322.86
	050.98	969.78	445.57	361.54	393.36	309.27
42	—	—	444.61	360.69	392.38	308.32
	049.31	967.56	443.13	359.10	390.80	306.77
	037.51	951.70	430.65	344.54	378.92	292.86
43	036.95	—	429.60	343.64	377.86	291.97
	036.27	949.81	428.13	342.13	376.29	290.47
	022.67	932.77	415.28	327.45	364.06	276.11
44	021.22	—	414.22	326.43	362.99	275.12
	019.85	931.14	412.75	324.87	361.45	273.52
	005.98	916.71	399.58	309.78	348.85	258.97
45	004.97	—	398.48	308.77	347.78	257.95
	003.44	915.78	397.05	307.27	346.23	256.43
	34989.33	899.14	383.47	291.88	333.25	241.52
46	988.48	897.66	382.36	290.62	332.16	240.46
	986.83	896.25	380.89	288.98	330.61	238.92
	972.23	879.65	367.01	—	317.31	223.60
47	971.44	878.76	365.90	—	316.15	222.50
	969.78	877.18	364.46	—	314.71	221.06
	955.06	860.41	350.20	—	301.04	205.42
48	—	859.53	349.01	—	299.88	204.25
	952.47	857.83	347.56	—	298.36	202.81
	936.91	840.66	333.06	—	284.49	186.83
49	936.08	839.82	331.75	—	283.14	185.67
	934.24	838.12	330.36	—	281.70	184.12
	35917.95	34820.77	34315.41	—	33267.36	33167.87
50	—	—	314.23	—	266.06	166.72
	916.71	818.20	312.72	—	264.67	165.24
	902.81	799.92	297.47	—	249.98	148.63
51	—	799.00	296.18	—	248.74	147.37
	899.98	797.32	294.71	—	247.25	145.99
	—	778.34	—	—	232.27	—
52	—	—	—	—	230.96	—
	881.98	777.30	—	—	229.38	—
	—	760.42	—	—	214.10	—
53	—	—	—	—	212.80	—
	—	757.64	—	—	211.41	—
	—	—	—	—	195.69	—
54	—	—	—	—	194.25	—
	—	—	—	—	192.85	—
	—	—	—	—	176.78	—
55	—	—	—	—	175.44	—
	—	—	—	—	174.02	—
	—	—	—	—	157.60	—
56	—	—	—	—	156.22	—
	—	—	—	—	154.62	—

TABLE I. (*Cont.*).

K''	(0, 6) λ3064.059 R	P	(0, 7) λ3164.761 R	P	(0, 8) λ3270.958 R	P	(0, 9) λ3383.114 R	P
5	—	—	—	—	30559.65	—	—	—
	—	—	—	—	560.89	—	—	—
	—	—	—	—	—	—	—	—
6	32624.35*	32611.17*	—	31572.68*	559.07	—	—	29533.82
	—	—	—	—	560.21	—	—	—
	—	—	—	—	—	—	—	531.72
7	622.85*	607.86*	—	569.22*	558.23	30543.42	29544.76	529.72
	—	—	—	—	559.65	—	546.24	—
	—	605.32	—	—	—	541.82	—	528.63
8	620.97*	604.17*	—	565.56*	556.90	540.00	543.59	526.35
	—	—	—	—	557.93	541.14	544.76	526.94
	—	601.71	—	563.53	555.28	538.31	541.38	524.95
9	618.45*	599.74*	—	561.51*	555.28	536.19	541.99	522.63
	—	—	—	—	555.93	537.08	542.73	522.91
	—	597.64	—	559.52	553.33	534.44	539.78	520.81
10	32616.05*	32595.05*	—	31557.18*	30553.07	30532.06	29539.78	29518.69*
	—	—	—	—	553.52	532.75	540.62	—
	—	593.08	—	555.21	550.99	530.20	538.04	517.15
11	613.14*	590.20*	31575.36*	552.48*	550.42	527.53	537.40	514.36*
	—	—	—	—	550.99	528.13	538.04	
	611.17	588.20	573.57	550.52	548.54	525.60	536.23	512.70
12	610.09*	585.04*	572.68*	547.46*	547.88*	522.59	534.65	509.69*
	—	—	—	—	—	523.05	535.53	
	607.86	583.00	570.55	545.49	545.66	520.67	532.78	507.92
13	606.54*	579.56*	569.22*	542.01*	544.55*	517.40	531.72	504.67*
	—	—	—	—	—	517.77	532.11	
	604.17	577.49	567.22	540.10	542.48	515.50	529.72	502.84
14	602.63*	573.67*	565.56*	536.39*	540.92*	511.89	528.63*	499.36*
	—	—	—	—	—	512.21		
	600.53	571.64	563.53	534.64	538.92	509.95	526.35	497.50
15	598.39*	567.49*	561.51*	530.73*	537.08*	506.34*	524.95*	493.89*
	596.29	565.65	559.52	528.57	535.04	504.16	522.63	491.71
16	593.82*	560.92*	557.18*	524.32*	532.99*	500.06*	520.81*	487.96*
	591.82	559.02	555.21	522.18	530.83	497.96	518.69	485.80
17	588.87*	554.04*	552.48*	517.63*	528.40*	493.56*	516.47*	481.68*
	586.86	552.05	550.51	515.49	526.28	491.41	514.36	479.46
18	583.68*	546.78*	547.46*	510.54*	623.54*	486.73*	511.86*	475.07*
	581.59	544.79	545.49	508.50	621.42	484.55	509.69	472.81
19	578.09*	539.21*	542.01*	503.15*	518.36*	479.55*	506.86*	468.09*
	576.04	537.03	540.10	501.08	516.18	477.42	504.67	465.86
20	572.08*	531.29*	536.39*	495.51*	512.87*	472.09*	501.57*	460.74*
	570.04	529.02	534.19	493.48	510.72	469.96	499.36	458.51
21	565.65*	523.07*	530.24*	487.45*	507.04*	464.28*	496.04*	453.14*
	563.71	520.86	528.17	485.41	504.88	462.11	493.89	450.95
22	559.02*	514.31*	523.87*	479.09*	500.92*	456.12*	490.08*	445.23*
	557.07	512.18	521.72	477.04	498.76	453.97	487.96	443.06
23	552.05*	505.36*	517.01*	470.35*	494.39*	447.66*	483.93*	437.07*
	550.15	503.09	514.98	468.28	492.28	445.49	481.68	434.89
24	32544.79*	32496.01*	31509.89*	31461.33*	30487.60*	30438.85*	29477.32*	29428.56*
	542.72	493.69	507.87	459.21	485.48	436.69	475.07	426.37
25	537.03*	486.32*	502.53*	451.94*	480.56	429.76*	470.52*	419.76*
					480 25			
	535.00	484.25	500.44	449.84	478.33	427.57	468.09	417.52
26	529.02*	476.27*	494.85*	442.17*	473.12	420.39	463.42	410.61*
					472.83	420.18	463.12	
	527.11	474.26	492.91	440.06	470.96	418.14	461.23	408.41
27	520.40*	465.89*	487.01	432.12*	465.36	410.66	455.93	401.15*
			486.65		464.97	410.36	455.59	
	518.54	463.83	484.65	429.99	463.10	408.38	453.57	398.92
28	511.67*	455.11*	478.58	421.75*	457.30	400.60	448.18	391.52
			478.19		456.89	400.27	447.76	391.19
	509.80	453.15	476.22	419.74	454.95	398.41	445.79	389.19
29	502.59*	444.08*	469.86	411.20	448.89	390.21	440.07	381.53
			469.38	410.79	448.38	389.82	439.65	381.10
	500.70	442.05	467.45	408.79	446.55	387.89	437.72	379.06

TABLE I. (Cont.).

K''	(0, 6) R	(0, 6) P	(0, 7) R	(0, 7) P	(0, 8) R	(0, 8) P	(0, 9) R	(0, 9) P
30	493.17*	432.70*	460.72	400.19	440.15	379.58	431.73	371.03
			460.24	399.72	439.61	379.06	431.16	370.65
	491.22	430.64	458.34	397.77	437.74	377.16	429.26	368.72
31	483.73	420.96*	451.29	388.73	431.04	368.46	422.95	360.34
	483.27		450.77	388.27	430.52	367.98	422.40	359.89
	481.44	418.86	448.90	386.38	428.59	366.10	420.47	357.93
32	473.69	409.04	441.55	377.02	421.62	357.07	413.91	349.28
	473.11	408.54	440.98	376.51	421.04	356.57	413.32	348.83
	471.30	406.74	439.13	374.60	419.24	354.69	411.42	346.91
33	463.24	396.66	431.45	365.00	411.95	345.41	404.59	337.95
	462.62	396.04	430.83	364.38	411.31	344.85	403.94	337.45
	460.76	394.25	429.03	362.61	409.47	342.93	402.03	335.56
34	452.39	383.84	420.97	352.53	401.90	333.47	394.87	326.41
	451.68	383.25	420.34	351.96	401.22	332.81	394.20	325.82
	449.94	381.45	418.56	350.20	399.38	330.95	392.33	323.90
35	441.22	370.72	410.20	339.80	391.50	321.23	384.89	314.47
	440.43	370.10	409.54	339.18	390.80	320.47	384.20	313.82
	438.70	368.35	407.79	337.38	388.97	318.58	382.31	311.92
36	32429.69	32357.29	31399.11	31326.73	30380.77	30308.50	29374.56	29302.18
	429.19	356.59	398.50	326.02	380.11	307.74	373.93	301.53
	427.20	354.82	396.64	324.26	378.26	305.88	371.97	299.63
37	417.89	343.35	387.70	313.27	369.72	295.49	363.99	289.56
	417.05	342.73	386.83	312.57	368.95	294.74	363.21	288.91
	415.27	341.01	385.12	310.78	367.14	292.89	361.31	287.02
38	405.48	329.26	375.80	299.54	358.33	282.14	352.95	276.72
	404.72	328.55	374.97	298.83	357.52	281.48	352.22	276.02
	403.10	326.80	373.24	296.92	355.72	279.49	350.32	274.08
39	392.94	314.77	363.68	285.46	346.60	268.47	341.71	263.51
	392.09	313.96	362.85	284.63	345.79	267.71	340.92	262.76
	390.41	312.23	361.13	282.87	344.08	265.84	338.99	260.87
40	380.03	299.87	351.15	271.00	334.55	254.42	330.08	249.89
	379.09	299.03	350.20	270.20	333.62	253.69	329.25	249.16
	377.49	297.31	348.58	268.44	331.94	251.83	327.42	247.30
41	366.69	284.63	338.32	256.20	322.16	240.08	318.15	236.09
	365.81	283.80	337.38	255.33	321.23	239.35	317.34	235.33
	364.17	282.09	335.80	253.68	319.58	237.59	315.47	233.43
42	353.12	268.99	325.21	241.15	309.57	225.43	306.01	221.96
	352.14	268.15	324.26	240.25	308.50	224.61	305.10	221.12
	350.48	266.49	322.59	238.55	306.86	222.90	303.26	219.32
43	339.13	253.09	311.72	225.59	296.52	210.39	293.46	207.44
	338.11	252.22	310.78	224.77	295.49	209.65	292.52	206.62
	336.52	250.67	309.06	223.10	293.88	207.94	290.77	204.82
44	324.78	236.83	297.84	209.91	283.16	195.13	280.56	192.70
	323.72	235.91	296.92	209.02	282.14	194.36	279.60	191.77
	322.16	234.26	295.21	207.28	280.48	192.63	277.83	189.98
45	310.10	220.23	283.65	193.79	269.48	179.60	267.43	177.58
	309.01	219.23	282.66	192.79	268.47	178.68	266.39	176.59
	307.47	217.65	280.98	191.25	266.80	177.00	264.67	174.88
46	295.04	203.26	269.15	177.32	255.46	163.66	253.93	162.14
	293.96	202.20	268.10	176.30	254.42	162.68	252.86	161.11
	292.40	200.68	266.44	174.76	252.76	161.01	251.06	159.42
47	279.64	185.98	254.27	160.49	241.18	147.52	240.15	146.49
	278.49	184.87	253.18	159.48	240.08	146.42	239.04	145.41
	276.96	183.30	251.55	157.85	238.40	144.77	237.31	143.69
48	263.87	168.27	239.07	143.37	226.50	130.89	225.98	130.40
	262.72	167.13	237.93	142.34	225.43	129.80	225.41	129.33
	261.16	165.60	236.36	140.66	223.73	128.16	223.20	127.54
49	247.84	150.21	223.56	125.94	211.52	113.97	211.61	114.01
	246.57	149.07	222.33	124.79	210.39	112.86	210.39	112.91
	245.10	147.52	220.81	123.12	208.72	111.17	208.71	111.34
50	32231.35	32131.85	31207.55	31108.10	30196.15	30096.68	—	—
	230.04	130.73	206.38	106.97	195.13	095.74	—	—
	228.62	129.17	204.85	105.37	193.35	093.93	—	—
51	214.54	113.20	191.25	090.09	180.51	079.13	—	—
	213.27	111.93	190.15	088.85	179.28	078.06	—	—
	211.84	110.42	188.53	087.28	177.68	076.33	—	—

TABLE I. (Cont.).

K''	(0, 6) R	P	(0, 7) R	P	(0, 8) R	P	(0, 9) R	P
	197.44	094.07	174.76	071.50	164.61	061.20	—	—
52	196.01	092.76	173.54	070.32	163.27	060.10	—	—
	194.41	091.31	171.84	068.76	161.51	058.53	—	—
	179.80	074.63	157.85	052.64	148.22	043.08	—	—
53	178.51	073.40	156.55	051.42	146.92	041.83	—	—
	177.06	071.93	155.05	049.89	145.37	040.25	—	—
	161.97	054.93	140.66	033.53	131.62	024.60	—	—
54	160.61	053.60	139.26	032.24	130.26	023.14	—	—
	159.17	051.96	137.79	030.53	128.74	021.39	—	—
	143.74	034.73	123.12	013.99	114.61	005.62	—	—
55	.42.40	033.43	121.69	012.70	113.26	004.23	—	—
	140.92	031.98	120.15	011.17	111.71	002.70	—	—
	125.19	014.28	105.16	30994.16	30097.25	29986.33	—	—
56	123.70	012.92	103.65	992.79	095.74	984.88	—	—
	122.34	011.50	102.19	991.26	094.35	983.39	—	—
	106.26	31993.45	086.80	974.03	079.62	966.76	—	—
57	104.76	992.04	085.35	972.64	078.06	965.31	—	—
	103.37	990.62	083.88	971.11	076.68	963.79	—	—
	086.96	972.26	068.17	953.48	061.65	946.81	—	—
58	085.43	970.85	066.70	952.08	060.10	945.38	—	—
	084.06	969.46	065.24	950.58	058.53	943.83	—	—
	067.34	950.76	049.16	932.61	043.08	926.64	—	—
59	065.86	949.27	047.71	931.14	041.83	925.26	—	—
	064.50	947.85	046.24	929.70	040.25	923.73	—	—
	047.40	928.83	029.90	911.37	024.60	906.13	—	—
60	045.63	927.34	028.20	909.91	023.14	904.69	—	—
	044.69	925.98	027.08	908.46	021.91	903.17	—	—
	027.05	906.57	010.25	889.89	005.62	885.23	—	—
61	025.38	905.13	008.62	888.36	004.23	883.82	—	—
	024.07	903.69	007.22	886.91	002.70	882.26	—	—
	006.25	884.04	30990.20	868.01	29986.33	864.10	—	—
62	004.66	882.40	988.55	866.31	984.88	862.43	—	—
	003.32	881.31	987.19	865.26	983.39	861.35	—	—
	31985.20	31861.10	30969.87	30845.81	29966.76	29842.60	—	—
63	983.61	859.54	968.19	844.22	965.31	841.00	—	—
	982.22	858.14	966.80	842.79	963.79	839.55	—	—
	963.82	837.81	949.14	823.20	946.81	820.69	—	—
64	—	836.14	947.53	821.55	945.38	819.06	—	—
	960.81	834.86	946.07	820.18	943.84	817.67	—	—
	941.95	814.11	928.08	800.27	926.29	798.54	—	—
65	—	812.49	—	798.67	924.70	796.96	—	—
	938.64	811.08	925.52	797.27	923.17	795.44	—	—
	—	790.10	—	776.95	—	776.05	—	—
66	—	788.55	—	775.40	—	774.46	—	—
	916.99	787.13	—	773.90	902.63	772.97	—	—
	—	765.72	—	753.37	—	753.14	—	—
67	—	764.27	—	—	—	—	—	—
	—	762.40	—	750.81	—	749.92	—	—
	—	—	—	—	—	—	—	—
68	—	—	—	—	—	—	—	—
	—	—	—	—	—	726.91	—	—

* These lines are made up of unresolved R_1 and R_3 (or P_1 and P_3) lines. The order in which the R branches are given is, reading downward, R_1, R_3, R_2. The same is true of the P branches.

The combination differences,

$$\Delta_2 F_i''(K) = R_i(K - 1) - P_i(K + 1) = F_i''(K + 1) - F_i''(K - 1)$$

for the lower electronic state have the same form as Eqs. (11), (12), and (13), except that the (′) is replaced by the (″). Because of lack of space, the numerical values of the combination differences are not given here. However, they can be obtained directly from the data in Table I. The values for a given

interval obtained from different bands agree, on the average, to about 0.06 cm^{-1}. The values of $\Delta_2 F_2(K)$, which are not a function of ϵ or γ, were used to determine the value of B_v. Graphs of $\Delta_2 F_2(K)/(K+\frac{1}{2})$ as ordinate with K as abscissa were made for all bands investigated. The ordinate at $K = -\frac{1}{2}$ is an approximate value of $4B_v$. Since

$$B_v = B_e - \alpha(v + \tfrac{1}{2}), \tag{14}$$

the difference between the values of B_v and B_{v+1} obtained from these graphs gave a preliminary value of α. The value of B_e was then calculated from Eq. (14) and substituted in the relation $D_e = -4B_e^3/\omega_e^2$ to obtain the value of D_e. D_v is given by the relation $D_v = D_e + \beta(v+\frac{1}{2})$, where $\beta = \alpha^2/6\omega_e + (20\alpha B_e^2 - 32x_e B_e^3)/\omega_e^2$. The value of D_v thus obtained can be used to calculate $8D_v(K+\frac{1}{2})^3$, which, when added to the observed values of $\Delta_2 F_2(K)$, yields a set of values $\Delta_2 F_2^*(K)$ which are practically linear in $(K+\frac{1}{2})$. $\Delta_2 F_2^*(K)$ is represented by

$$\Delta_2 F_2^*(K) = \Delta_2 F_2(K) - 8D_v(K + \tfrac{1}{2})^3 = 4B_v(K + \tfrac{1}{2}). \tag{15}$$

The least squares solution of this equation gives an accurate value of $4B_v$. The values of $4B_v$ thus obtained were fitted to Eq. (14) by the least squares method to obtain B_e and α.

The values of the molecular constants obtained from the data given above are listed in Table II.

TABLE II. *Constants of the rotational structure.*[15]

v'	B_v'	Constants	v''	B_v''	Constants
0	0.4989	$B_e' = 0.5020 \pm 0.0005$ cm^{-1}	4	0.68367	$B_e'' = 0.70894 \pm 0.00009$ cm^{-1}
1	0.4927	$\alpha_e' = 0.0062$ cm^{-1}	5	0.67793	$\alpha_e'' = 0.005622 \pm 0.000013$ cm^{-1}
		$I_e' = 55.10 \times 10^{-40}$ gr. cm^2	6	0.67248	$I_e'' = 39.02 \times 10^{-40}$ gr. cm^2
		$r_e' = 1.769 \times 10^{-8}$ cm	7	0.66674	$r_e'' = 1.489 \times 10^{-8}$ cm
		$D_e' = -1.280 \times 10^{-6}$ cm^{-1}	8	0.66124	$D_e'' = -1.129 \times 10^{-6}$ cm^{-1}
		$\beta' = -3.56 \times 10^{-9}$ cm^{-1}	9	0.65548	$\beta'' = -3.20 \times 10^{-10}$ cm^{-1}

Band	A	B	$\gamma' - \gamma''$
(0,4)	-1.97	-10.83	+0.0150
(0,5)	-2.02	"	"
(0,6)	-2.06	"	"
(0,7)	-2.09	"	"
(0,8)	-2.11 ± 0.01	" ± 0.01	" ± 0.0005
(0,9)	-2.19	"	"

	$\gamma' \sim +0.017$		$\gamma'' \sim -0.003$

Note: As mentioned later in the text, the signs of γ', γ'', and $(\gamma' - \gamma'')$ are somewhat arbitrarily chosen.

IV. SPIN FINE STRUCTURE OF THE ROTATIONAL LEVELS

As pointed out above, the existence of three energy levels for each value of K is to be attributed to the mutual interaction of the individual spins com-

[15] The constants A, B, and γ are discussed in the following section. The values of r_e are calculated for the molecule $S^{32}O^{16}$, since these are by far the most abundant of the isotopes of these elements.

bined with the interaction of the resultant spin S^* and the magnetic field generated by nuclear rotation. The separations of these levels from the energy given by $B_vK(K+1)+D_vK^2(K+1)^2+\cdots$ are represented by Eqs. (6), (7) and (8). The rotational term differences are expressed by Eqs. (11), (12), and (13). If the terms in ϵ in these equations are neglected, as they may be except at low K, then

$$\Delta_2F_1(K) - \Delta_2F_3(K) = 4\gamma. \tag{16}$$

The value of 4γ is, in the present case, less than the experimental error; hence, for any one value of K, Eq. (16) does not give even an approximate value of γ, and the average for a large number of K values gives only a rough approximation. The values of γ' and γ'' were determined from each of the six bands with $v'=0$ by averaging all the available differences $\Delta_2F_1(K)$ $-\Delta_2F_3(K)$ for $K>25$. The values of γ' thus obtained ranged from $+0.025$ to $+0.011$ with an average $+0.017$. The values of γ'' ranged from -0.006 to -0.0006 with an average -0.003. No consistent variation of γ'' with v'' was observed. Although these values of γ' and γ'' represent only the order of magnitude of the correct values, they appear to be definitely of opposite sign. However, the above data alone are insufficient to determine whether γ'' is negative or positive, since we do not know which of the two high-frequency R (or P) branches is the theoretical R_1 (or P_1) branch.

It has been shown that the value of γ''[16] for the normal $^3\Sigma_g^-$ state of the O_2 molecule is negative,[13] and that the value of γ' for the excited $^3\Sigma_u^-$ state for the Schumann-Runge bands of O_2 also is negative.[8] For this reason, Naudé and Christy[9] have assumed that the values of γ for the normal $^3\Sigma_g^-$ and the excited $^3\Sigma_u^-$ states of S_2 also are both negative, since both have the same sign. A similar situation in SO, however, does not exist, since the sign of γ for the normal $^3\Sigma$ state is opposite to that for the excited $^3\Sigma$ state. If we assume that the sign of γ'' for SO is the same as that for the normal states of O_2 and S_2, then the designation of the high-frequency R (or P) branch as R_1 (or P_1) is correct.

The equations for the separations of the three components of the triplet in the R and P branches, obtained from Eqs. (9) and (10) are:

$R_1 - R_3 = 6\epsilon'(2K + 3)/(2K + 5)(2K + 1)$
$\qquad\qquad - 6\epsilon''(2K + 1)/(2K + 3)(2K - 1) + (\gamma' - \gamma'')(2K + 1) + 2\gamma'$ (17a)

$R_2 - R_1 = 3(\epsilon' - \epsilon'') - 3\epsilon'/(2K + 5) + 3\epsilon''/(2K + 3)$
$\qquad\qquad - (\gamma' - \gamma'')(K + 1) - \gamma'$ (18a)

$R_2 - R_3 = 3(\epsilon' - \epsilon'') + 3\epsilon'/(2K + 1) - 3\epsilon''/(2K - 1) + (\gamma' - \gamma'')K + \gamma'$ (19a)

$P_1 - P_3 = 6\epsilon'(2K - 1)/(2K + 1)(2K - 3)$
$\qquad\qquad - 6\epsilon''(2K + 1)/(2K + 3)(2K - 1) + (\gamma' - \gamma'')(2K + 1) - 2\gamma'$ (17b)

$P_2 - P_1 = 3(\epsilon' - \epsilon'') - 3\epsilon'/(2K + 1) + 3\epsilon''/(2K + 3)$
$\qquad\qquad - (\gamma' - \gamma'')(K + 1) + \gamma'$ (18b)

$P_2 - P_3 = 3(\epsilon' - \epsilon'') + 3\epsilon'/(2K - 3) - 3\epsilon''/(2K - 1) + (\gamma' - \gamma'')K - \gamma'$ (19b)

[16] The γ used here corresponds to $(-B)$ in Kramers' terminology (cf. reference 13) and to $(-D)$ in that of Lochte-Holtgreven and Dieke (cf. reference 8).

For $K \geqq 5$, the average of Eqs. (18a) and (18b) is:[17]

$$\Delta_{2-1} = 3(\epsilon' - \epsilon'') - 3(\epsilon' - \epsilon'')/(2K + 3) - (\gamma' - \gamma'')(K + 1) \qquad (20)$$

and the average of Eqs. (19a) and (19b) is:[17]

$$\Delta_{2-3} = 3(\epsilon' - \epsilon'') + 3(\epsilon' - \epsilon'')/(2K - 1) + (\gamma' - \gamma'')K. \qquad (21)$$

The interval between R_2 and the mean of R_1 and R_3, for K greater than about 5,[17] is:

$$\Delta_{2-1,3} = 3(\epsilon' - \epsilon'') - \tfrac{1}{2}(\gamma' - \gamma''). \qquad (22)$$

This interval is the same for the corresponding P branches.
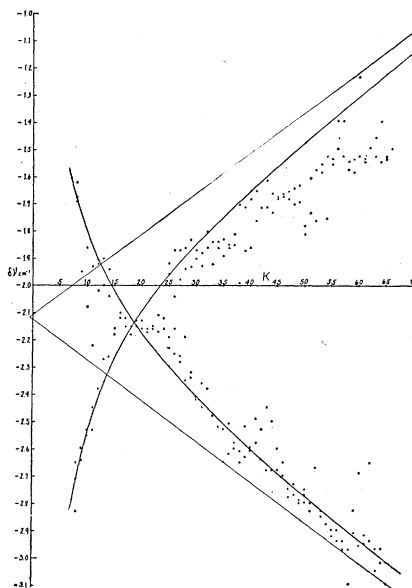
Fig. 3. Graphs showing the triplet separations in the 0,8 band. The ordinates for the circles and triangles represent, respectively, the observed separations of R_1 and R_3 from R_2, and of P_1 and P_3 from P_2. The curves are plotted according to Eqs. (23) and (24), where $A = -2.11$, $B = -10.83$, and $(\gamma' - \gamma'') = +0.0150$. These curves approach asymptotically the straight lines whose slopes are $\pm(\gamma' - \gamma'') = \pm0.0150$.

The R_1 and R_3 (and P_1 and P_3) branches are resolved for $K > 30$, and, in some cases, for $K < 13$. The resolution for $K < 13$ was most satisfactorily observed in the (0,8) band, since this band showed very little overlapping of the different branches in the region of small K values. Accordingly, in order to determine the tripling constants as accurately as possible, the separations of the three components of the triplets of the (0,8) band were plotted on a large scale (Fig. 3). The circles and triangles represent, respectively, the wave-number separations of R_1 and R_3 from R_2, and P_1 and P_3 from P_2.

[17] These equations contain approximations of the type $(1/(2K+5))$ $(1/(2K+1)) \sim (1/(2K+3))^2$, which are not very good for very low values of K.

According to Kramers' theory of spin tripling in $^3\Sigma$ states,[13] Eqs. (20) and (21) should represent the observed separations of the members of the triplets, at least for the smaller values of K. However, it was found that it was impossible to represent the data by using the same value of $3(\epsilon' - \epsilon'')$ in both of the first two terms of Eqs. (20) and (21). The equations which best represent the data for the (0,8) band, for low values of K, are:

$$\Delta_{2-1} = A - B/(2K + 3) - (\gamma' - \gamma'')(K + 1) \tag{23}$$

$$\Delta_{2-3} = A + B/(2K - 1) + (\gamma' - \gamma'')K \tag{24}$$

where $A = -2.11$, $B = -10.83$, and $(\gamma' - \gamma'') = +0.0150$. Since there is at present no theoretical interpretation of this discrepancy, which also occurs in the $^3\Sigma_g^-$ normal state of O_2,[18] we cannot determine which one, if either, of two terms, A and B, represents the value of $3(\epsilon' - \epsilon'')$ in Kramers' theory.
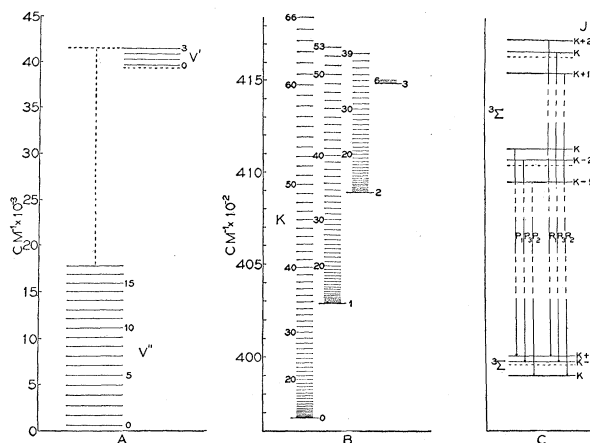
Fig. 4. Energy-level diagram. (A). The vibrational levels of the upper and lower $^3\Sigma$ states. No levels with $v'>3$ are observed. (B). The rotational levels of the upper state. This shows the values of K' at which the bands are observed to break off. (C). A schematic representation of the structure of the rotational levels of the two $^3\Sigma$ states. Only the levels associated with the lines $R(K)$ and $P(K)$ are shown. The separations of the actual levels from those which would exist if there were no spin are indicated qualitatively by the displacements of the full from the dashed lines.

The curves in Fig. 3 represent graphs of Eqs. (23) and (24) with the appropriate values of the constants A, B, and $(\gamma' - \gamma'')$. These curves approach asymptotically the straight lines whose slopes are $\pm(\gamma' - \gamma'') = \pm 0.0150$, and whose common intercept at $K = -\frac{1}{2}$ is $A - \frac{1}{2}(\gamma' - \gamma'') = -2.125$. The difference between the ordinates of the straight lines and of the corresponding curves represents the value of the terms containing K in the denominator in Eqs. (23) and (24). The data for low K values are represented well within experimental error, but for large K the data deviate considerably from sym-

[18] R. T. Birge and H. H. Nielsen, unpublished work on the atmospheric oxygen bands. The writer is indebted to Professor Birge for the methods used in the determination of the constants A, B, and $(\gamma' - \gamma'')$.

metry about the horizontal line $\delta\nu = -2.125$ cm^{-1}, due undoubtedly to the fact that the energy of interaction of S* and the magnetic field generated by the rotation of the molecule deviates appreciably from the linear form assumed in setting it equal to $\gamma(K^* \cdot S^*)$.[19]

The wave-number separations of the members of the triplets were plotted for all six bands with $v' = 0$, and the constants A, B, and $(\gamma' - \gamma'')$ were determined from them as accurately as possible. On account of the fact that overlapping prevented complete resolution of the branches at low K values for bands other than the (0,8), the constants obtained from these bands are undoubtedly less accurate than those obtained from the latter.

A schematic representation of the structure of the rotational levels is shown in Fig. 4c. Only the levels associated with the lines $R(K)$ and $P(K)$ are shown. The displacement of the actual levels from those which would exist if the spin were absent is indicated qualitatively by the displacements of the full from the dotted lines.

V. Predissociation and Perturbations

An unusual feature of the bands under consideration, and one which has considerable theoretical significance, is the abrupt termination of the band system at a certain definite value of the initial vibrational quantum number, namely $v' = 3$. It will be evident from the matrix diagram of Fig. 8 that no bands with $v' > 3$ are observed. The phenomenon is analogous to that found in the emission bands of S_2[9] and P_2,[20] and has been shown to be the result of predissociation. Furthermore, the rotational structure of the individual bands is found in all of the SO bands to break off suddenly at a particular value of K', the rotational quantum number in the upper state. This value is large for bands with $v' = 0$, but decreases with increasing v', and is very small for $v' = 3$.

The abrupt termination of the rotational structure of the (0,7) band is shown in Fig. 2d, while similar effects in the (2,2), (2,3), and (3,3) bands can be seen in Fig. 2c. The (3,3) band is extremely narrow, and so faint that it is difficult to observe on the enlargement, although it was easily visible on the original plates. Two other bands with $v' = 3$, which also present the same appearance, can also be seen on the original plates.

It has been shown by Bonhoeffer and Farkas,[21] and by Kronig,[22] that, if the discrete energy levels of an electronic state lie above the dissociation limit of another electronic state, there is, according to the quantum mechanics, a certain probability that a molecule in one of these levels will undergo a radiationless transition to the other electronic state, and dissociate spontaneously. This transition must obey certain selection rules derived by Kronig, and, if the conditions of the Franck-Condon principle are fulfilled, the probability

[19] R. S. Mulliken, Rev. Mod. Phys. **2**, 105 (1930) and references given there, especially J. H. Van Vleck, Phys. Rev. **33**, 467 (1929).

[20] G. Herzberg, Nature **126**, 239 (1930).

[21] K. F. Bonhoeffer and L. Farkas, Zeits. f. Physik Chem. **(A)134**, 337 (1927).

[22] R. de L. Kronig, Zeits. f. Physik **50**, 347 (1928); **62**, 300 (1930).

that such a transition will occur may be very great. In this case, the life-time of the molecule in the discrete levels can become comparable with, or smaller than, the period of nuclear rotation. Accordingly, if these levels belong to the upper electronic state, the lines involving them will be diffuse in absorption, and either faint or absent in emission. This phenomenon is known as predissociation.[23]

Since the vibrational levels are spaced on a larger scale than the rotational levels, predissociation usually shows itself in absorption by the fact that the bands of the v' progressions become diffuse at a certain value of v', as was first observed in the S_2[24] spectrum. In emission, the same band progressions will terminate abruptly at this value of v'. The energy of this critical level represents, in some cases, the dissociation limit of the state which is causing the predissociation, and hence the phenomenon permits an evaluation of the heat of dissociation of the molecule. When the rotational structure is well resolved, as in the present case, observations on the exact value of the rotational quantum number at which the break occurs may lead to a very precise value of the heat of dissociation, and also give information of a new type concerning the mechanism of the process. The only case of this kind which has heretofore been studied is that of P_2,[20] where the resolution is less complete, and the details have not yet been published.

The K' values[25] of the last lines of the bands with $v' = 0$, and $v' = 1$, were found by application of the combination principle to be 66 and 53 respectively. However, the rotational levels for $v' = 2$ were too much perturbed, and those for $v' = 3$ too few, to permit an analysis of the rotational structure of bands involving these levels. Accordingly , the K' values of the last lines of these bands were determined from the wave-number difference between the head and last line of the band in question by means of Eq. (10), where B_v' and B_v'' were obtained from Eq. (14). These values of K' were found to be 39 for $v' = 2$, and 6 for $v' = 3$, but may be in error by one or two units.

The observed energy levels of the SO molecule are shown in Fig. 4; (A) shows the vibrational levels of both states, and (B) shows the rotational levels of the upper state. The rotational levels for different values of v' break off not only at different K values, but also at different energy values, and the energy at which the break occurs decreases with increasing v'. According to the interpretation of this effect given below, the term value at which the $v' = 3$ levels break off ($41,520$ cm^{-1}) probably corresponds to dissociation of the lower electronic state. Linear extrapolation of the vibrational levels of the lower state gives $51,620$ cm^{-1} as the term value corresponding to dissociation. However, it is well known that this extrapolation practically always leads to values which are considerably too large.[26]

[23] For a general discussion of predissociation, see G. Herzberg, Erg. exakt. Naturwiss. 10, 207 (1931).

[24] V. Henri, Jour. Phys. Rad. 3, 181 (1922); Structure of Molecules (1925).

[25] The use of K, instead of J, is justified by the fact that the three energy levels for a given K are much closer together than those with the same J.

[26] R. T. Birge, Nat'l. Research Council Bulletin on Molecular Spectra, (1926).

The oxygen atom and the sulphur atom each have a ^3P normal state and a ^1D first excited state. The energy of excitation of this ^1D state of oxygen is given by Frerichs[27] as 1.95 volts, and that of sulphur is estimated by Christy and Naudé[28] as 1.60 volts. Linear extrapolation of the vibrational levels of the excited state of SO leads to 56,840 cm^{-1} as the term value corresponding to dissociation of this state. If the convergence limit 41,520 cm^{-1} is subtracted from this limit at 56,840 cm^{-1}, we have 1.89 volts as the energy of atomic excitation. Although linear extrapolation of the levels of the excited state is especially untrustworthy in view of the fact that so few levels are observed, and that these levels may be perturbed, it seems probable that 1.89 volts is too high; therefore, we may assume that the sulphur atom is excited, and that 1.60 volts represents the energy of excitation. In this case, the dissocia-
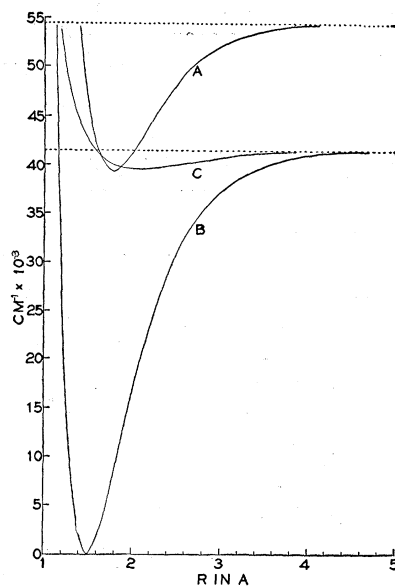
Fig. 5. Potential energy curves of the SO molecule. Curves A and B represent the two known $^3\Sigma$ states, and are plotted according to Morse's equation. Curve C ($^3\Pi$) has been assumed in order to account for predissociation.

tion limit of the excited $^3\Sigma$ state is at about 54,400 cm^{-1}, instead of 56,840 cm^{-1}, as obtained by linear extrapolation. Since this ^1D level is the first excited atomic state upon which the upper $^3\Sigma$ state of the molecule can be built, the dissociation limit at 41,520 cm^{-1} must represent dissociation into two normal ^3P atoms, and, therefore, dissociation of the normal state of the SO molecule.

Potential energy curves for the known states of the SO molecule are shown in Fig. 5; curves A and B represent the upper and lower $^3\Sigma$ states for

[27] R. Frerichs, Phys. Rev. **36**, 398 (1930).

[28] A. Christy and S. M. Naudé, Phys. Rev. **37**, 903 (1931), obtained the value for S by interpolation from the known values for O, Se, and Te atoms.

the observed bands, and are plotted according to Morse's[29] equation, while curve C must be assumed in order to account for predissocation. The electronic states represented by A and B are both $^3\Sigma$, and probably both $^3\Sigma^-$, since this is the case in O_2 and S_2. The molecule in state B is built of two ^3P atoms, and in state A of a ^3P and a ^1D atom. Since ^1D is the lowest excited atomic state, the molecule in state C, in order that C may cause predissociation, must also be built of two ^3P atoms. The possible electronic states of a molecule composed of two dissimilar ^3P atoms are:[30] two $^1\Sigma^+$, $^1\Sigma^-$, two $^1\Pi$, $^1\Delta$, two $^3\Sigma^+$, $^3\Sigma^-$, two $^3\Pi$, $^3\Delta$, two $^5\Sigma^+$, $^5\Sigma^-$, two $^5\Pi$, and $^5\Delta$. The selection rules for a radiationless transition of a molecule composed of two dissimilar atoms, as given by Kronig,[22] are: $\Delta\Lambda = 0$, ±1; $\Delta\Sigma$ and $\Delta S = 0$; $\Delta J = 0$; the transition can occur only between two rotational levels which are both positive or both negative. Accordingly, of the electronic states listed above, the only ones which can interact with the upper $^3\Sigma^-$ state are the $^3\Pi$ and the $^3\Sigma^-$ states. In addition to Kronig's selection rules, there is another requirement which must be fulfilled for two electronic states to be able to interact to any noticeable degree;[23] the potential energy curves of the two states must approach each other very closely. As shown in Fig. 5, the curves for the two $^3\Sigma^-$ states are everywhere well separated; hence these states cannot interact enough to cause predissociation. Therefore, the interacting state must be $^3\Pi$.

Herzberg[23] has suggested that the decrease with increasing v' of the term value at which the rotational levels break off, which was also observed in P_2,[23] is an effect of rotation of the molecule, and that an explanation is to be found by an application of the same principles which Oldenberg used to interpret the dissociation by rotation alone which occurs in the HgH bands.[31]

If we represent the potential energy of the molecule by $U(r)$, the force acting on the nuclei is given by $U'(r)$, the derivative of $U(r)$ with respect to the internuclear distance r. If the molecule is allowed to rotate, but not vibrate, it will expand to a new equilibrium position, such that the centrifugal force is equal to the attractive force; then $p^2/\mu r^3 = U'(r)$, where p is the angular momentum of the nuclei, and μ is their reduced mass. If the molecule then vibrates about this new position of equilibrium, with constant angular momentum, it will be acted upon by a restoring force $U'(r) - p^2/\mu r^3$. This force can be represented by the derivative with respect to r of the expression $U(r) + p^2/2\mu r^2$. The expression $p^2/2\mu r^2$ is equal to the kinetic energy of rotation of the molecule; or

$$T(r) = p^2/2\mu r^2 = BK(K + 1) + DK^2(K + 1)^2 + \cdots \tag{25}$$

Hence, with the assumption that the angular momentum is constant, $U(r) + T(r)$ is an "effective" potential energy, and has the same meaning for

[29] P. M. Morse, Phys. Rev. **34**, 57 (1929).

[30] R. de L. Kronig, Band Spectra and Molecular Structure (Cambridge), (1930); R. S. Mulliken, Rev. Mod. Phys. **4**, 1 (1932); E. Wigner and E. E. Witmer, Zeits. f. Physik **51**, 859 (1928).

[31] O. Oldenberg, Zeits. f. Physik **56**, 563 (1929). In the case of the HgH bands, the effect was due entirely to dissociation by rotation of the molecule in the lower electronic state, while in the present case, a radiationless electronic transition is involved.

a vibrating and rotating molecule that $U(r)$ has for a molecule which is vibrating, but not rotating.

As required by the Franck-Condon principle, $T(r)$ must be added to the $U(r)$ curve of each of the interacting states, and a radiationless transition can occur between only those $U(r) + T(r)$ curves which have the same $T(r)$ (i.e., same angular momentum). Accordingly, the shape of the $^3\Pi$ curve determines the intersections of its $U(r) + T(r)$ curves with those of the upper $^3\Sigma^-$ state, and, therefore, the term values at which the rotational levels break off. If the $^3\Pi$ state is assumed to be repulsive for all values of r, as Christy and Naudé[28] assumed for S_2, the decrease with increasing v' of the term value at which the rotational levels break off would be much greater than is observed. In order to satisfactorily explain the observed facts, it was necessary to assume a shallow minimum in the $^3\Pi$ curve, as shown in Fig. 5 (curve C).
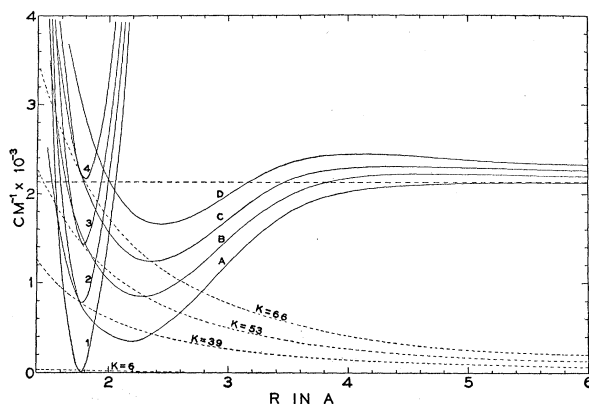
Fig. 6. *Effective* potential energy curves for the $^3\Pi$ and upper $^3\Sigma$ states for various amounts of rotation. The dashed curves represent the kinetic energy of rotation of the molecule, $T(r)$ $= p^2/2\mu r^2$, for the K values indicated. Curves 2, 3, and 4 are obtained by adding the dashed curves to curve 1. Curves B, C, and D are obtained from A similarly. The horizontal dashed line, according to our interpretation, corresponds to the energy of dissociation of the $^3\Pi$ and lower $^3\Sigma$ states.

In Fig. 6, $U(r) + T(r)$ curves are plotted for states A (upper $^3\Sigma^-$) and $C(^3\Pi)$ of Fig. 5 for the four values of K' at which the rotational levels for the different values of v' are observed to break off. The dashed curved lines represent graphs of $T(r) = p^2/2\mu r^2$, where p, for a given K', has been evaluated from Eq. (26) by using B_e', D_e', and r_e'. Curves 1 and A of Fig. 6 correspond to curves A and C of Fig. 5 respectively, but are on a much larger scale. Curves 1 and A have also been taken to represent $U(r) + T(r)$ for $K = 6$, since $T(r)$, in this case, is negligibly small for the values of r with which we are concerned here. Curves 2, 3, and 4 are obtained by adding the dashed curves $(T(r))$ to curve 1 $(U(r))$; curves B, C, and D are obtained from A similarly. The horizontal dashed line represents the term value at which the rotational levels for $v' = 3$ are observed to break off.

If the molecule is in the upper $^3\Sigma^-$ state, and is rotating with $K = 6$, its

potential energy is represented by curve 1, and, if in addition it is vibrating with $v' = 3$, it has an energy corresponding to the horizontal dashed line. Accordingly, as the molecule vibrates along curve 1, it can undergo, at the points of intersection of 1 and A, an electronic transition, without any change of internuclear distance and momentum, from $^3\Sigma^-$ to $^3\Pi$, and begin vibrating along curve A. Since the molecule has sufficient energy, it vibrates along A to large r and dissociates. If $K' = 66$, the molecule vibrates along curve 4, and can undergo a transition to curve D at the point of intersection. In this case, only the vibrational energy corresponding to $v' = 0$ is required for the molecule to be able to pass the hump at large r in curve D and dissociate.

The Franck-Condon principle allows only the following transitions between the curves shown in Fig. 6: 1 to A, 2 to B, 3 to C, and 4 to D. These are the transitions which the molecule undergoes when it dissociates with $v' = 3$, 2, 1, and 0, respectively. If the molecule has only the vibrational energy corresponding to $v' = 0$, then, in order to dissociate, it must also have rotational energy corresponding to $K' = 66$. For $K' > 66$, the molecule can also dissociate, and, if the probability that this will occur is sufficiently great, spectrum lines involving these levels will not be observed in emission. A similar argument applies to the other vibrational levels.

The fact that the height of the hump at large r in the $U(r) + T(r)$ curves of the $^3\Pi$ state increases with increasing rotational energy requires the total (vibrational plus rotational) energy necessary for predissociation to increase with decreasing vibrational energy. Accordingly, the rotational levels for $v' = 0$ break off at a term value greater than those for other v' levels by just the difference in the heights of the humps in the corresponding $U(r) + T(r)$ curves of the $^3\Pi$ state. If we assume that the $^3\Pi$ state has the $U(r)$ curve shown in the figures, the agreement between the heights of these humps and the term values at which the rotational levels for the various values of v' are observed to break off is quite satisfactory.

As mentioned above, the $^3\Pi$ state cannot be repulsive for all values of r, because its $U(r) + T(r)$ curves would then intersect those of the $^3\Sigma^-$ state with the same angular momentum considerably above the dissociation limit of the $^3\Pi$ state (except for small angular momentum), with the result that the decrease with increasing v' of the term value at which the rotational levels break off would be much greater than is observed. In order than an appreciable interaction between the $^3\Pi$ and upper $^3\Sigma^-$ states shall occur, the potential energy curves for these states must intersect.[23] Accordingly, the minimum in the $^3\Pi$ curve must occur at large r and be shallow, which means a low frequency of vibration. As drawn in the figures, the curve obeys the empirical rule of Morse:[29] $\omega_e r_e^3 \sim 3000 \times 10^{-24}$ cm^2.

A further indication that the $^3\Pi$ curve has a shallow minimum is given by the observed perturbations of the rotational levels of the upper $^3\Sigma^-$ state. Since perturbations of the type observed in the present case are the result of interaction of two electronic states which have discrete levels of nearly the same energy, they indicate, as shown below, that the $^3\Pi$ state cannot be repulsive for all values of r.

Only a few of the rotational levels for $v' = 0$ are perturbed; these perturbations consist of displacements of only a single level from its expected position. The only noticeable perturbations occur at $K' = 53$ and 61, where the F_2 levels only are displaced from their expected positions. The perturbation at $K' = 61$ can be seen in Fig. 2d; it occurs in the P_2 branch in the sixth member from the right of the figure, and in the R_2 branch in the second member from the left. This type of perturbation indicates that the levels of the perturbing state are spaced quite differently than those of the perturbed $^3\Sigma^-$ state.

The rotational levels for $v' = 1$, however, are considerably perturbed. Fig. 2e, is an enlargement of part of the (1,4) band, and shows very clearly the irregularities of the rotational structure. As can be seen in the figure, the lines occur in distinct groups, where each group is composed of the lines $P(K)$ and $R(K+5)$. The difference in appearance of successive groups is so great, however, that it is impossible to distinguish the R from the P lines by inspection. The identification and proper numbering of the lines in terms of K'' were obtained from term differences for the lower electronic state.
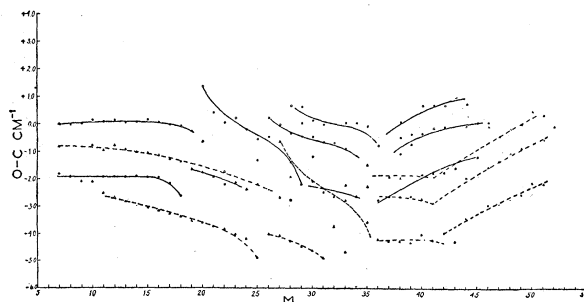
Fig. 7. Perturbations in the rotational structure of the 1,4 band. The ordinate represents the difference between the observed wave numbers of the lines and the wave numbers calculated from a formula of the type, $\nu = a + bM + cM^2 + dM^3$. The circles and triangles refer to R and P lines, and the full and dashed curves represent the general course of the R and P branches, respectively. M is equal to K'' for the P branches, and to $K'' - 5$ for the R branches. The band is quite regular up to $K' = 23$, but thereafter the perturbations are complex.

Any regularities which are present in the band can be discovered by fitting the edges of the groups to an equation of the type $\nu_M = a + bM + cM^2 + dM^3$, where M is an integer. The differences between the observed wave numbers of the lines and the wave numbers calculated from this equation are shown in Fig. 7 as ordinate with M as abscissa. M is equal to K'' for the P branches (represented in the figure by dashed lines), and $K'' - 5$ for the R branches (solid lines). The similarity of the curves for the R and P branches is apparent. For $K'' < 23$, the band is fairly regular, but, for $K'' > 23$, the perturbations are large and complex. Because of this complexity, only the general course of the branches is represented by the curves in this region.

The rotational levels for $v' = 2$ are so much perturbed that an analysis of the structure of bands involving these levels could not be made. Similarly, nothing can be said concerning perturbations of the levels for $v' = 3$, since only about 6 rotational levels are present, and the bands are very weak.

Since the rules governing states which can interact to cause perturbations[22] are identical with those for predissociation, the only states which can perturb the upper $^3\Sigma^-$ state are the $^3\Pi$ and lower $^3\Sigma^-$ states, however, the potential energy curves of the $^3\Sigma^-$ states do not approach each other very closely; it therefore seems very improbable that these states could interact enough to cause perturbations of the magnitude observed. Hence the $^3\Pi$ state must be causing the perturbations. If this is the case, its potential energy curve, as stated above, must have a minimum. That the minimum is shallow is indicated by the fact that there are no perturbations of levels whose term values are less than that corresponding to $v' = 1$, $K' = 23$, while above this point there are many. It should be mentioned that it is possible, although it does not seem probable, that some other molecular state built on a normal and an excited atom is causing the perturbations.

Since both the perturbations and predissociation observed in the rotational structure require the $^3\Pi$ potential energy curve to have a shallow minimum, the curve must lie approximately as drawn in the figures. In this case, one would expect to observe discrete bands resulting from transitions from the $^3\Pi$ state to the lower $^3\Sigma^-$ state. However, the molecule in this $^3\Pi$ state would spend most of its time at large values of r; therefore, the most intense bands would occur at longer wave-lengths than those of the $^3\Sigma^-$, $^3\Sigma^-$ system. These bands have not been observed. Perhaps the continuum underlying the observed bands is an indication of the presence of this state.

Herzberg[23] has pointed out that the abruptness of the termination of the bands is an indication of the accuracy with which heats of dissociation can be determined by this method. If the bands terminate very abruptly, as in the present case, a very good value of the energy of dissociation can be obtained. According to the above interpretation of predissociation of the SO molecule, the term value at which the rotational levels for $v' = 3$ break off corresponds to dissociation of the normal state. If the energy of dissociation is measured from the $v'' = 0$ vibrational level, it is calculated from the relation

$$D'' = \nu_e - G_0'' + G_0' + \Delta G_{\frac{1}{2}}' + \Delta G_{1\frac{1}{2}}' + \Delta G_{2\frac{1}{2}}' + F'_{v'=3}(6) \qquad (26)$$

to be 5.053 ± 0.001 volts. (See next section for the values of these terms, except $F_{v'=3}'$ (6), which is calculated from Eq. (5).) This result for D'' is considerably less than the value 6.42 volts obtained by Henri and Wolff by linear extrapolation of the vibrational levels. The uncertainty of 0.001 volt in our value is due principally to inaccuracy in the determination of the value of K' at which the rotational levels for $v' = 3$ break off. Provided our interpretation of the phenomenon is correct, the accuracy of this value of the energy of dissociation of SO is equal to that of the most precise determination of energy of dissociation by any method, namely the spectroscopic value for I_2.[32]

If we assume that the excited $^3\Sigma^-$ state is built on a normal oxygen atom and a sulphur atom excited with 1.60 volts of energy, its energy of dissociation, measured from the $v' = 0$ vibrational level, is 1.83 volts. The $^3\Pi$ state,

[32] W. G. Brown, Phys. Rev. **38**, 709 (1931).

according to our interpretation, has an energy of dissociation of the order of 0.2 volt.

VI. VIBRATIONAL STRUCTURE

The wave-lengths and estimated intensities of the band heads are given in the $v'v''$ diagram in Fig. 8. These values were taken from the work of Henri and Wolff.[3] The fact that the left and upper sides of this diagram are sharply bounded by fairly intense progressions is a good indication that this assignment of vibrational quantum numbers is correct, although the assignment of v' is more certain than that of v''. The solid curve is drawn through the most intense bands of the system, and thus indicates the observed most probable changes of the vibrational quantum number. The dashed curve represents the most probable changes predicted by an application of the Franck-Condon principle, using potential energy curves plotted according to Morse's equation. The agreement between the two curves is as good as could be expected,

v' \ v''	0	1	2	3	4	5	6	7	8	9	10	11	12	13	14
0	2555.5	2630.1	2708.6	2791.0	2877.4	2968.4	3064.1	3164.7	3271.0	3383.2	3502.3	3628.2	3761.6	3903.6	
1	2516.4	2589.0	2664.8	2744.3	2827.8	2915.4	3007.9			3314.8	3428.1	3548.7	3676.2	3811.8	3941.6
2	2477.7	2548.6	2622.2	2699.4	2779.9				3247.5				3774.7	3952.7	
3	2442.0	2510.4	2581.1	2655.7											
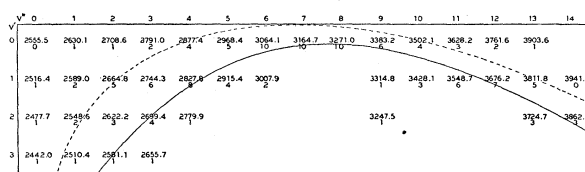
Fig. 8. This $v'v''$ matrix diagram gives the wave-lengths and estimated relative intensities of the heads of the bands of the SO spectrum. These values are taken from the work of Henri and Wolff. The solid curve is drawn through the most intense bands of the system, and thus indicates the observed most probable changes of the vibrational quantum number. The dashed curve indicates the most probable changes predicted by an application of the Franck-Condon principle, using potential energy curves plotted according to Morse's equation.

in view of the fact that the predicted values were determined from classical, instead of wave-mechanical, transition probabilities, and that the observed intensities are merely visual estimates of photographic density. The rapid decrease of plate sensitivity at the short wave-length end of the spectrum is probably responsible for the fact that, in this region, the observed curve lies below and to the right of the predicted curve.

Henri and Wolff obtained values of ω_e'', ω_e', and $x_e''\omega_e''$, but, due to inaccuracies of measurement, could not get the value of $x_e'\omega_e'$. In the present work, the origins of the six bands of the $v'=0$ progression which were measured were calculated by means of Eq. (9), using the R_2 branches. (In this calculation, the constant A of Eqs. (23) and (24) was arbitrarily taken to represent the value of $3(\epsilon' - \epsilon'')$.) From these origins, the values of ω_e'' and $x_e''\omega_e''$ were determined with much greater accuracy than is afforded by measurements of band heads only. The wave numbers of the origins and the vibrational term differences, $\Delta G_v''$, are given in Table III. The differences, $\Delta G_v''$ observed, were fitted to the equation:

$$\Delta G_v'' = \omega_e'' - 2x_e''\omega_e''(v'' + \tfrac{1}{2}), \qquad (26)$$

using least squares formulas. The values thus obtained are: $\omega_e'' = 1123.73$

± 0.24 cm^{-1}, and $2x_e{}''\omega_{e''} = 12.232 \pm 0.034$ cm^{-1}. The values of $\Delta G_v{}''$ calculated from Eq. (26) are recorded in Table III as $\Delta G_v{}''$ calc., and the differences between the observed and calculated values are given as $O - C$.

Due to perturbations of the rotational levels, it was not possible to determine accurately the origins of bands with $v' > 1$. Therefore, in order to obthe values of $\omega_e{}'$ and $x_e{}'\omega_e{}'$, it was necessary to use measurements of band heads. Table III also gives the wave-lengths and wave-numbers of the heads of the bands used for this purpose, and the values of $\Delta G_v{}'$.

TABLE III. *Band heads, band origins, and vibrational term differences.*

Band	ν_0 cm^{-1}	$\Delta G_v{}''$ Obs.	$\Delta G_v{}''$ Calc.	$O - C$
(0, 4)	34736.31			
		1062.62	1062.57	+0.05
(0, 5)	33673.69			
		1050.20	1050.34	−0.14
(0, 6)	32623.49			
		1038.28	1038.10	+0.18
(0, 7)	31585.21			
		1025.74	1025.87	−0.13
(0, 8)	30559.47			
		1013.69	1013.64	+0.05
(0, 9)	29545.78			

Band	λ_h I.A.	ν_h cm^{-1}	$\Delta G_v{}'$	Band	λ_h I.A.	ν_h cm^{-1}	$\Delta G_v{}'$	Av. $\Delta G_v{}'$
(0, 3)	2791.33	35814.7		(0, 4)	2877.66	34740.4		
			617.5				617.3	617.4
(1, 3)	2744.02	36432.2		(1, 4)	2827.41	35357.7		
			606.3				605.6	606.1
(2, 3)	2699.10	37038.5		(2, 4)	2779.79	35963.3		
			606.1					
(3, 3)	2655.64	37644.6						

The fact that the values of $\Delta G_v{}'$ for the $v'' = 3$ progression are not linear shows that at least one of the upper state vibrational levels is perturbed. Since the $v' = 3$ level is very close to the dissociation limit of the lower state, it was considered as more likely to be perturbed than any of the others. Therefore, only the values of $\Delta G_v{}'$ obtained from the levels with $v' = 0$, 1, and 2 were used in the determination of the vibrational constants of the upper state. In getting the average $\Delta G_{1\frac{1}{2}}{}' = 606.1$, the value 606.3 was given greater weight than 605.6, since the position of the head of the (2,4) band was difficult to measure. The average $\Delta G_v{}'$ values thus obtained give $\omega_e{}' = 628.7$ cm^{-1}, and $2x_e{}'\omega_e{}' = 11.3$ cm^{-1}. Because of the fact that these were obtained from only two values of $\Delta G_v{}'$, no probable error for them can be given, although it seems quite likely that they may be in error by a few tenths of a wave number.

The vibrational term values of the upper state are given by:

$$G_v{}' = 628.7(v' + \tfrac{1}{2}) - 5.65(v' + \tfrac{1}{2})^2 \qquad (27)$$

and those of the lower state by:

$$G_v{}'' = 1123.73(v'' + \tfrac{1}{2}) - 6.116(v'' + \tfrac{1}{2})^2. \qquad (28)$$

The origin of the band system was calculated from the relation $\nu_e = \nu_0 + G_v'' - G_v'$, where ν_0 represents the origin of the (v', v'') band, and G_v' and G_v'' are obtained from Eqs. (27) and (28). The average ν_e obtained from the seven bands investigated is 39356.3 cm^{-1}.

The writer takes this opportunity to express his sincere appreciation of the invaluable suggestions given to him by Professor F. A. Jenkins, under whose supervision this investigation has been conducted.

Fig. 2. Reproduction of the major parts of the SO emission spectrum, photographed with a 21-foot grating. (a) and (b). Contact prints of the region λ2500A to λ3550A, which contains most of the stronger bands. (c). Enlargement of the short wave-length end of the spectrum to show the abrupt termination of the bands with $v' = 2$ and $v' = 3$. This is especially well illustrated by the 2,2 band. The 3,3 band is probably too faint to show in the reproduction, but actually is only about 1 mm wide. (d). Enlargement of the end of the 0,7 band showing the abrupt ending of the R and P branches. (e). Enlargement of part of the 1,4 band illustrating the perturbations in the rotational structure. (f). Enlargement of part of the 0,5 band. The complete resolution of the triplets and their different relative spacing for adjacent lines, $R(K)$ and $P(K-6)$, are apparent.